JOURNAL GEOLOGICAL SOCIETY OF INDIA
Vol.92, July 2018, pp.11-18

Genesis of the Sulfide Hosted Refractory Gold Occurrences within the Carbonaceous Metasedimentary Units of the Dalma Volcano-sedimentary Basin, North Singbhum Mobile Belt, Eastern India

Mousoma Khatun and Sahendra Singh*
Department of Applied Geology, Indian Institute of Technology (Indian School of Mines), Dhanbad - 826 004, India
***E-mail**: sahendrasingh02@gmail.com*

ABSTRACT

Paleo-Mesoproterozoic (1.0-2.4 Ga) north Singhbhum mobile belt (NSMB) is one of the prominent polymetallic mineral belt within the Singhbhum crustal province of eastern India lying between Chotanagpur gneissic complex (CGC) in the north and the Archaean Singhbhum craton (>2.4 Ga) in the south. The study area is located along the northern fringe of Dalma volcano-sedimentary basin. Lithological variations, structure, metamorphism and tectonic setting indicate good prospect for regional gold exploration within this area.Extensive work by Geological Survey of India (GSI) within this basin reveals gold occurrences with its concentrations ranging from 0.1 to 4 ppm within the carbonaceous cherty quartzite. Gold mineralization within the area has been reported to be associated with quartz ± quartz carbonate vein either as disseminated gold or as refractory gold within the sulfides. A detailed study on the occurrence of refractory gold associated with carbonaceous cherty quartzite has not been carried out by any of the previous workers. The present work report the occurrence of refractory gold associated with sulfides within the carbonaceous host rocks. Detailed petrographic studies of the carbonaceous host rock reveal the presence of sulfides such as pyrrhotite, pyrite, chalcopyrite, arsenopyrite. EPMA studies of the host rocks indicate the presence of invisible gold within the sulfides varying in concentration from 100 to 1000 ppm. Total organic carbon (TOC), high resolution X-ray diffraction (HR-XRD) and Fourier transform infrared spectrometry (FTIR) analysis show the presence of organic carbon within the samples. Presence of organic carbon facilitates reducing environment required for gold mineralization within carbonaceous host rock in the study area.

INTRODUCTION

The term 'invisible gold' was first introduced by Burg (1930) and has been defined as the presence of gold as colloidal sizes in solid solution. Previous studies suggest various modes of origin for invisible gold such as sub-microscopic metallic particles or as ''chemically bound'' gold (Cabri et al. 1989,1991; Cathelineau et al.1989; Cook and Chryssoulis 1990; Friedl et al.1995; Fleet and Mumin 1997; Genkin et al. 1998, Maddox et al. 1998). Recovery processes for the invisible gold are difficult, due to their very small sizes (i.e. $<10^4$ AÚ to ≤2.8 AÚ) and also due to the lack of understanding regarding its occurrence with sulfides (Yang et al.1998). "Invisible gold" occurrences are more commonly associated with hydrothermal gold deposits (Simon et al. 1999; Palenik et al. 2004; Large et al.2009). Boyle (1980, 1987) suggested that arsenopyrite and pyrite are the major host minerals for invisible gold.

In recent years, nano-particles of gold or invisible gold have drawn attention because of its large application in biomedical and technological industries due to its unique photonic, electric and catalytic property (Hough, 2011). Proper understanding of the lattice bound gold with the help of advance technology may lead to the identification hidden gold prospect areas within Dalma volcano-sedimentary basin (Jha et al. 2015). Further studies of "invisible gold" enhance our knowledge to recover gold from sulfides (Hough, 2011). Concentration of invisible gold in study area is higher in pyrrhotite compared to other sulfides, such types of association has been previously reported from other VMS deposits (Galley et al. 2007).

North Singhbhum mobile belt (Fig.1) has attracted the attention of exploration geologist during the last decades as many gold prospects were reported from various parts of the belt (Pal et al. 2010; Jha et al. 2015).The mobile belt is divided into five lithotectonic domains i.e., Dhanjori-Chaibasa, Singhbhum Shear Zone, Dhalbhum, Dalma and Chandil Formation (Mahadevan, 2002) (Fig.2). Dalma volcano-sedimentary belt belongs to the fourth domain and has the characteristics of a typical greenstone belt (Gupta et al. 1980, 2000). Based on structural and geochemical signature of volcanic rocks, previous workers have proposed a probable evolutionary model for Dalma volcano-sedimentary basin. Most of these workers have suggested the development of basin in a mantle plume activated intercontinental rift setting (Gupta et al.1982; Mukhopadhaya 1990, 1994; Erriksson et al. 1999; Mazumder, 2000; Roy et al. 2002b; Mazumder, 2003). Mantle upwelling over this greenstone belt has made it one of the most important metallogenetic province of eastern India (Zhang et al. 2008; Wan et al. 2010). Geophysical studies show high conductivity contrast along with high resistivity and magnetic anomaly and significant radiometric anomaly in the study area indicating rift margin type of tectonic setting (Maurya et al. 2015). The worldwide association of gold deposits within the greenstone belt makes the Dalma basin a potential target for gold prospects (Saha and Venkatesh, 2002). The study area is also well known for placer gold occurrences along Subarnarekha river and its tributaries (Jha et al. 2015).

In this work petrographic studies, scanning electron microscope (SEM) analysis, and electron probe micro analyzer (EPMA) studies of sulfides within the carbonaceous cherty quartzite were carried out in order to understand the occurrence of invisible gold in association with the sulfides. Studies related to gold occurrences have also been carried out by previous workers (Maurya et al. 2015). Refractory gold occurrences within the carbonaceous chert have also been reported from Paleoproterozoic (~1800 Ma) Dariba-Rajpura-Bethumni belt of Rajasthan (Pal et al., 2013).

0016-7622/2018-92-1-11/$ 1.00 © GEOL. SOC. INDIA | DOI: 10.1007/s12594-018-0947-1

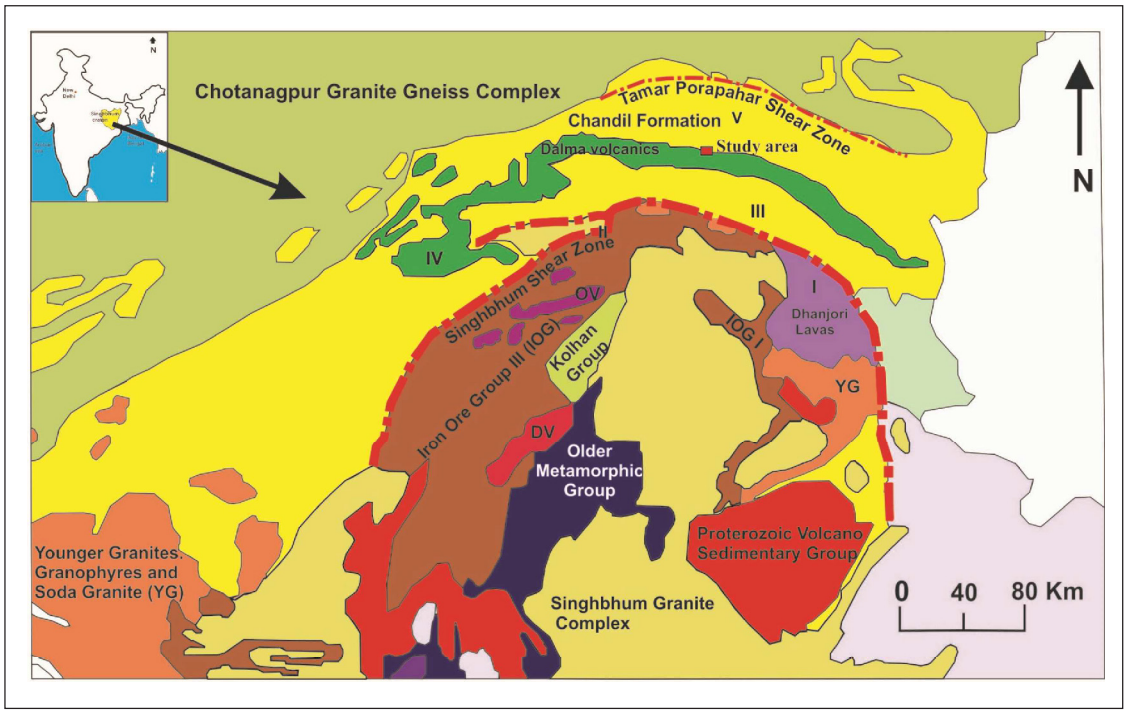

Fig.1. Regional geological map of Singhbhum crustal province with the study area location (modified after Geological map of India, 7th edition, 1998).

GEOLOGICAL SETTING

North Singhbhum mobile belt shows evidences of complex interplay of sedimentation and tectonism (Bhattacharya and Mahapatra, 2008) and suggests multiple phases of reactivation during Paleo and Mesoproterozoic periods (Mishra and Johnson, 2005; Mahato et al., 2008). The region is traversed by two major crustal scale shear zones. The northern shear zone, which is also known as south Purulia shear zone, demarcates NSMB from Chotanagpur granitic gneissic complex (CGGC) (Chatterjee et al., 2013) at its northern margin. Singhbhum shear zone lies along the southern margin of NSMB. Dalma volcano-sedimentary belt has a strike length of 200 km and width varying from 3 to 7 km. The basin exhibit an arcuate synclinal feature trending E-W (Mahadevan, 2002). Presence of thrusted contact between Dalma and Chandil Formation has been reported by several workers (Dunn 1929; Dunn and Dey, 1942). The region exhibits post-depositional compressional deformation of volcano-sedimentary sequence, which ranges from greenschist to amphibolite facies of metamorphism. Dalma volcano-sedimentary basin dominantly comprises of volcanic and volcanoclastic rocks with interbeds of quartzite and phyllites at some places (Yellur, 1977; Bhattacharya and Dasgupta, 1979; Gupta et al., 1980, 1982; Chakraborti, 1980; Chakraborti and Bose, 1985; Bose et al., 1989; Singh, 1997, 1998; Mazumder, 2005). The two fold lithostratigraphic division of this domain has been proposed by previous workers (Gupta et al.1980,1982). Lower Dalma Formation comprises of mafic and acidic pyroclastic rock whereas upper Formation is distinguished by ultramafic to mafic lava flows. Whole rock isochron of gabbro pyroxenite intrusive of Dalma volcanic by Rb-Sr method yielded an age of 1619±38 Ma (Roy et al., 2002b; Mazumder, 2005).

The study area (Fig. 3) comprises of carbonaceous cherty quartzite, mica schist, carbonaceous phyllites, weakly metamorphosed felsic volcanic rocks and volcanoclastic rocks. Bedding planes are preserved in carbonaceous phyllites. Alternate bands of cherty quartzite and carbonaceous phyllites are present.

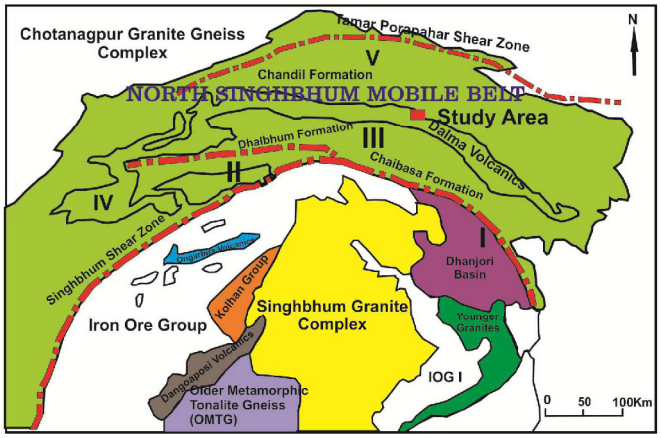

Fig.2. Schematic map of North Singhbhum Crustal Province exhibiting various lithostratigraphic domains of the province with study area (modified after Sarkar S.C. et al., 1992;Gupta and Basu, 2000).

PETROGRAPHY AND ORE MINERALOGY OF CARBONACEOUS HOST ROCK

Petrographic characterization of carbonaceous host rocks were carried out in the Ore Geology Laboratory, Indian Institute of Technology (Indian School of Mines), Dhanbad. Carbonaceous cherty quartzite and carbonaceous phyllites occur as alternate bands (Fig.4a). Structural features such as intraformational fold were observed within the carbonaceous cherty quartzite at some places (Fig.4b). Petrographic studies of carbonaceous cherty quartzite reveal presence of quartz, muscovite, carbonates (mainly calcite) sericites, epidote, monazite and dusty carbonaceous matter (Fig.4c). Carbonaceous cherty quartzite are massive as well as laminated and are defined by the presence of lithic grains associated with carbonaceous detritus and lack of mat like laminations (Walsh et al. 1999). Carbonaceous matter present within these cherty quartzites are wisps, diffuse and in some places crystalline. Partially flattened wisps in carbonaceous matters are most common. These carbonaceous layers are folded at some places (Fig.4d). Quartz veins are also present within carbonaceous cherty quartzite with their thickness varying from few mm to cm and show cross cutting relationship at places. Microstructural evidences such as

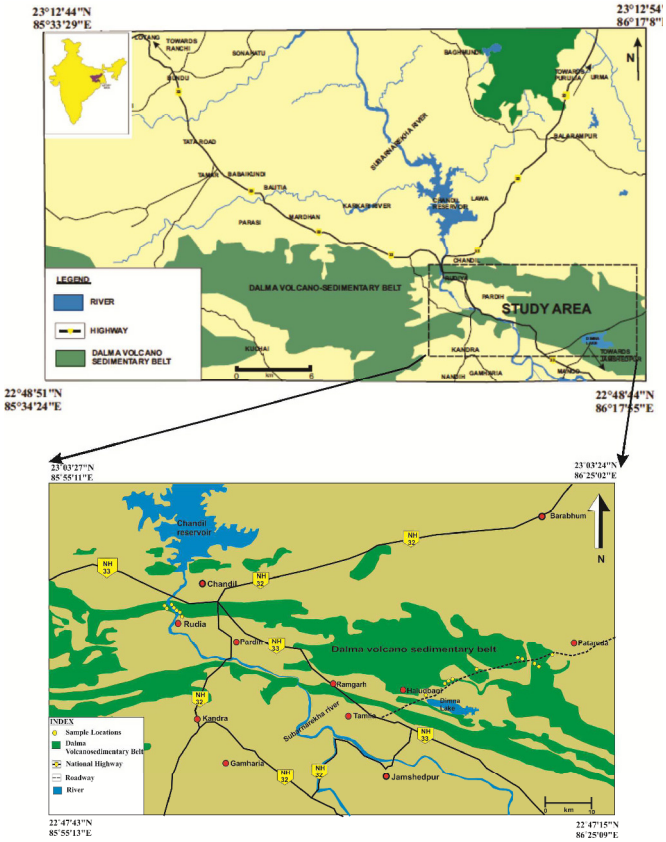

Fig.3. Sample locations and accessibility of study area in satellite imagery.

ptygmatic folding, faulting and shearing of quartz veins imply that the area has undergone intense deformation and metamorphism (Fig.4e).

Ore minerals associated with the mineralized quartz carbonate veins (Fig.4f) are pyrite, pyrrhotite, magnetite, hematite, chalcopyrite, arsenopyrite and goethite. Pyrite and pyrrhotite both occur as dominant sulfide phase. Pyrites are mostly euhedral (Fig.4e) and in some places anhedral with suture or serrated grain boundary which indicates variable degree of dissolution (Keith et al., 2016). Pyrrhotite appears as a stretch lineation (Fig.4g). At some places it has been replaced by chalcopyrite and magnetite (Fig.4i,j). Disseminated zoned pyrite is present within the host rocks (Fig.4k). Pyrite is also present as inclusions within the pyrrhotite (Fig.4k). Presence of goethite within these rocks indicates supergene enrichment in study area. Martitization (Fig.4l) of magnetite is due to oxidation at surface condition.

MINERAL CHEMISTRY AND THE CHARACTERIZATION OF SULFIDES

Chemical analyses of sulfide within the carbonaceous cherty quartzite were performed using electron probe micro analyse (EPMA) and scanning electron microscope (SEM)-EDS facility of Central Research Facility (CRF), Indian Institute of Technology (ISM), Dhanbad. EPMA was performed on a CAMECA SX-five model. A probe current of 10 µA at an accelerating voltage of 30 kV and a beam size of 600 nm were used. The counting time maintained was 10 seconds. Detection limit for sulfides was 100 ppm. SEM-EDS analysis was carried out in Carl –Zeiss Supra-55. The chemical data of sulfides are given in Table 1.

SEM-EDS study confirms pyrrhotite and pyrite present as the abundant phases within the litho unit (Fig.5).A substantial amount of invisible gold has been detected within the sulfides ranging from 100 ppm-1000ppm. Pyrrhotite predominantly host the invisible gold compared to other sulfides. Apart from invisible gold, silver (Ag) is also present with its concentration ranging from 100-600ppm (Table 1). EPMA analysis was carried out on pyrrhotite, pyrite, arsenopyrite, chalcopyrite grains (Fig.6). Invisible gold in pyrrhotite ranges from 100-1000 ppm.In chalcopyrite it is 1000 ppm, In pyrite it ranges from 400-600 ppm whereas in arsenopyrite it is around 600 ppm. Similarly silver ranges from 100-400 ppm in pyrrhotite, around 700 ppm in pyrite and 400-600 ppm in arsenopyrite (Table 1).

CHARACTERIZATION OF CARBON WITH THE HELP OF FTIR, TOC AND HR-XRD ANALYSIS

FTIR analysis is helpful in the characterization of organic bond in the rock samples (Chen et al. 2012). To carry out FTIR analysis, the host rocks were finely powdered and subjected to HCL→HF treatment digestion for total eviction of silicates and carbonates. In this procedure about 5 grams of powdered samples were taken. The carbonates were removed by 6N hydrochloric acid, and then clay minerals, quartz and silicates were decomposed twice by using a mixture of 40% HF and 6N HCl. The first lasted for 4 hours, and the second was performed overnight, then the moistened residue was repeatedly washed with distilled water for several times. This process was further followed by residue, dried in oven at constant temperature with an end product of pure carbonaceous matter (Vandenbroucke 2003). During pellet preparation for FTIR analysis, a small fraction of the carbonaceous matter was added with KBr (Sahoo et al. 2014; Russell 1987). FTIR analysis was carried out at Sophisticated Analytical Instrumentation Facility (SAIF), IIT Mumbai using 3000 Hyperion Microscope with Vertex 80 FTIR System, Bruker, Germany. The IR spectra were manipulated with spectrum 2000 software and reported in transmittance units as function of wave number (cm^{-1}) in the 3500-500 cm^{-1} range. The spectral band assignment was chosen after Okolo et al. (2015) and Chen et al. (2012).

FTIR analysis of carbonaceous cherty quartzite and carbonaceous phyllite shows distinct peaks at 1579,1672 cm^{-1} for aromatic C=C stretching, 1020,1087cm^{-1} for aliphatic skeletal C-C; C-O stretching; and –OH bending vibration, 2916 cm^{-1} symmetric aliphatic CH_3 stretching vibration, whereas in some samples it shows a peak around 1618 cm^{-1} which indicates presence of aromatic C=C stretching, –OH stretching vibration defined by peak position at 3622-3696 cm^{-1} (Fig.7a,b)

To evaluate organic carbon characterization total organic carbon (TOC) analysis plays a vital role. For determination of total organic carbon, carbonaceous host rock were finely powdered and treated with concentrated HCL for 24 hours in Teflon beaker. The carbonate carbon was removed in the form of carbon dioxide. For this experiment a constant temperature of 50°C was maintained and regularly stirred for total removal of carbonate carbon. Then residue decarbonated moistened samples was washed repeatedly and dried in oven. To carry out this analysis, untreated samples were analyzed first to obtains total carbon (TC) and then treated decarbonated samples were analyzed to obtain total organic carbon (TOC). The analysis was carried out by LECO (CHN628) Analyzer at NML (National Metturalgical Laboratory), Jamshedpur.

TOC analysis shows presence of organic carbon from 1.08 to 5.72 wt% for carbonaceous phyllite whereas in carbonaceous cherty quartzite it ranges between 0.02 to 6.98 wt% (Table 2).

High Resolution XRD (HR-XRD) analysis carried out for identifying mineral phases at Indian Association for Cultivation of Science, Kolkata. HR-XRD analysis showed presence of carbon, quartz, clay minerals and muscovite in host rock (Fig. 8).

SITING OF INVISIBLE GOLD WITHIN SULFIDES

The presence of invisible gold in the lattice structure of sulfides suggest the role of hydrothermal fluids in gold precipitation. Concentration of invisible gold varies within sulfides. Maximum being

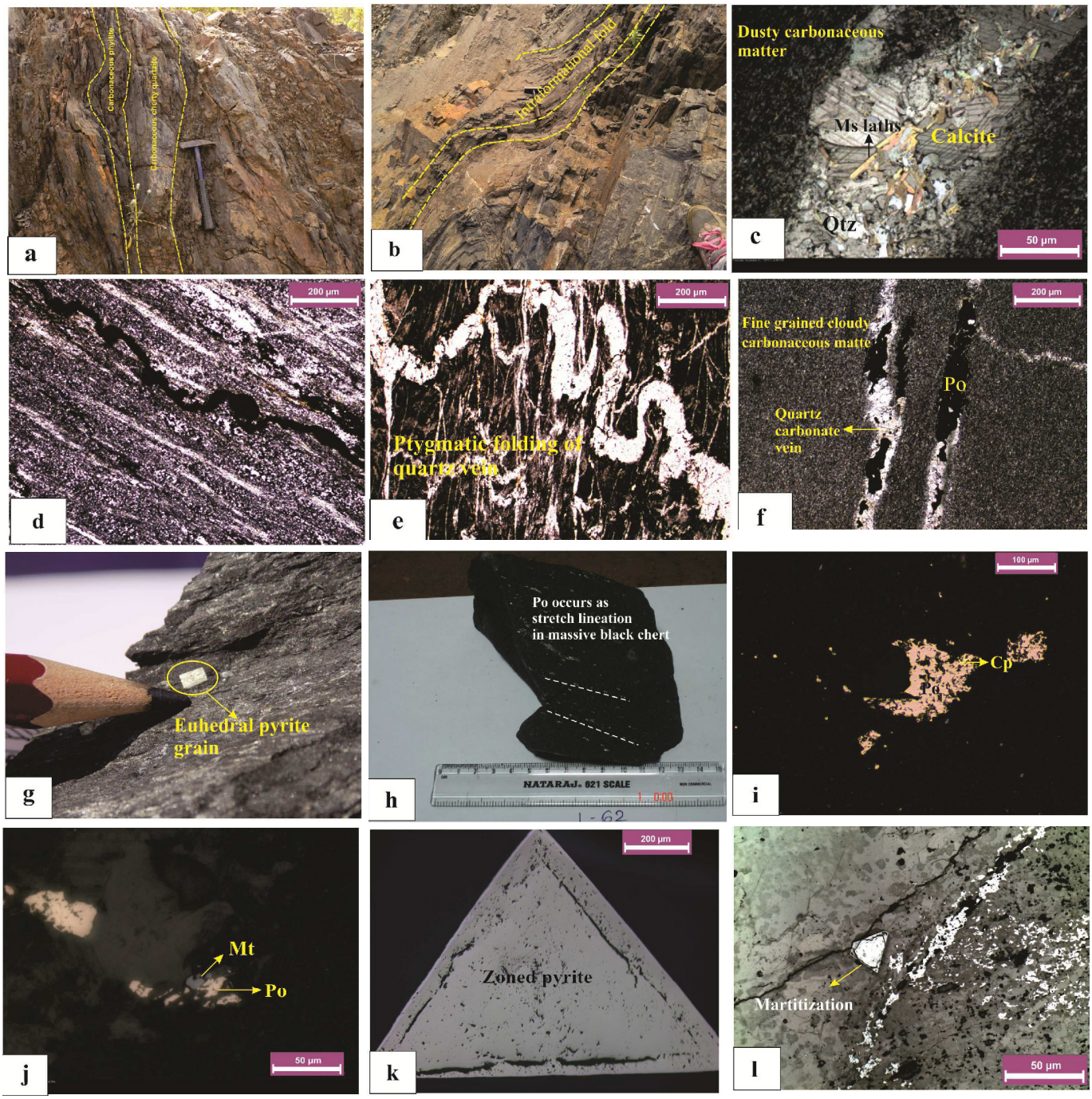

Fig.4. Field photograph showing(a) Alternate layers of carbonaceous cherty quartzite and carbonaceous phyllite(b)Intraformational fold found within cherty quartzite layer Photomicrograph showing (c) Calcite and muscovite laths present along quartz carbonate veins with dusty carbonaceous matter in carbonaceous cherty quartzite (d) Folding of carbonaceous matter within laminated black cherty quartzite. (e) Ptygmatic fold of quartz vein indicates deformational evidence, Photomicrograph showing (f) Ore mineralization occurs within quartz carbonate veins,Hand specimen photo showing (g) Euhedral pyrite within host rock (h) Pyrrhotite occurs as a stretch lineation in host rock, Photomicrograph showing (i) Pyrrhotite replaced by chalcopyrite (j) Pyrrhotite replaced by magnetite(k)Zoned pyrite grain (l)Martitization.

in pyrrhotite and chalcopyrite (1000ppm) and followed by arsenopyrite (600ppm) and pyrite (400-600ppm).Variation in invisible gold content in some samples imply its heterogeneous distribution. Higher concentration of invisible gold within the pyrrhotite indicate its occurrences as a solid solution within sulfides and also suggest that the deposition of gold has taken place at higher temperature (Sahoo, 2011). Possibilities of introduction of invisible gold from latter gold bearing solution in sulfides are rejected because of the refractory nature of sulfides. (Saha and Venkatesh, 2002).

Various theories were proposed to understand the occurrences of invisible gold within crystal lattices of sulfides. Substitutional mechanism reveals that Au replaces As sites because of their similar radii when covalently bonded (Boyle, 1980). Some studies state that Au enrichment takes place with relative depletion of Fe (Tarnocai et al., 1997). Au has a negative valence state in arsenopyrite and pyrite as it substitutes S atoms or chemically bound with S by covalent bond (Li et al., 1994). In Hutti-Maski gold deposit of South India, Au precipitated as invisible gold within sulfides by the substitution of Fe^{3+} by Au^{3+} (Saha and Venkatesh, 2002). In our study area, the possible mechanism for invisible gold deposition is explained by the substitution of Fe by Au within the sulfides as it is present within arsenopyrite and also other sulfides containing Fe cations (as evident

Table 1. Mineral chemistry of selected sulphide minerals detected by EPMA (Values of S,Fe, Cu, Co,Ni,As,Sn in wt% and Au, Ag,Bi,Pb in ppm)

Sl No.	Mineral	Composition	S	Fe	Cu	Co	Ni	As	Ag	Au	Pb	Bi	Sn	Total
1 / 1	Po	$Fe_{(1-x)}S_x$	37.88	60.79	0	0.03	0.1	0.08	100	700	800	0	0.02	99.7
2 / 1	Po	$Fe_{(1-x)}S_x$	37.88	59.78	0	0.06	0.07	1	0	100	800	700	0.02	99.84
3 / 1	Po	$Fe_{(1-x)}S_x$	37.88	60.26	0	0.07	0.11	0	100	0	1900	200	0.07	99.11
4 / 2	Po	$Fe_{(1-x)}S_x$	37.88	60.27	0	0.03	0.09	0.36	300	700	700	1800	0.04	99.36
5 / 2	Po	$Fe_{(1-x)}S_x$	37.88	60.19	0	0.08	0.1	0.38	0	200	200	0	0	99.42
6 / 2	Po	$Fe_{(1-x)}S_x$	37.88	60.24	0.02	0.04	0.1	0.49	300	0	0	2200	0.01	99.38
7 / 3	Po	$Fe_{(1-x)}S_x$	37.88	59.71	0	0.04	0.17	0.13	100	0	0	1100	0	98.42
8 / 3	Po	$Fe_{(1-x)}S_x$	37.88	59.72	0.04	0.07	0.12	0	400	0	800	1800	0.04	97.49
9 / 3	Po	$Fe_{(1-x)}S_x$	37.88	60.09	0	0.03	0.13	0.29	0	0	100	200	0.05	99.31
10 /4	Po	$Fe_{(1-x)}S_x$	37.88	59.8	0.01	0.08	0.12	0	0	0	2300	1000	0	99.22
11 /5	Po	$Fe_{(1-x)}S_x$	37.88	59.97	0.01	0.02	0.13	0.46	0	200	1500	900	0.03	99.73
12 /6	Po	$Fe_{(1-x)}S_x$	37.66	60.14	0	0.09	0.15	0.01	0	0	1900	1900	0.02	98.95
13 /6	Cp	$CuFeS_2$	34.70	29.44	32.38	0	0	0.12	0	1000	700	700	0.01	97.32
14 /6	Po	$Fe_{(1-x)}S_x$	36.56	56.08	0	0.02	0.14	0	0	700	600	1600	0	93.76
15 /6	Po	$Fe_{(1-x)}S_x$	37.91	60.54	0	0.05	0.13	0	0	0	1600	1800	0.04	99.47
16 /7	Py	FeS_2	52.16	44.74	0.13	2.42	0.01	0	700	100	1400	2400	0.02	100.38
17 /7	Po	$Fe_{(1-x)}S_x$	39.35	59.19	0.01	0.03	0.14	0	0	100	300	2200	0	99.32
18 /7	Po	$Fe_{(1-x)}S_x$	38.29	60.25	0	0.07	0.16	0	0	0	300	1400	0	99.20
19 /7	Po	$Fe_{(1-x)}S_x$	38.07	59.49	0	0.08	0.14	0.21	300	0	1700	1700	0.04	98.94
20 /7	Po	$Fe_{(1-x)}S_x$	38.94	58.95	0	0.06	0.18	0	100	0	1800	600	0	98.78
21 /7	Py	FeS_2	52.25	47.13	0.01	0.02	0.01	0	100	200	0	2300	0.01	100.08
22 /7	Py	FeS_2	53.58	47.28	0	0.02	0.12	0	0	0	1300	3200	0	101.86
23 /7	Po	$Fe_{(1-x)}S_x$	37.73	59.8	0	0.07	0.18	0	100	0	1400	1100	0.05	98.57
24 /7	Py	FeS_2	52.94	47.02	0	0.06	0.1	0.24	0	0	800	1500	0.02	101.25
25 /7	Py	FeS_2	52.80	45.61	0.03	0.02	0.01	0.53	0	0	100	2100	0	100.08
26 /7	Po	$Fe_{(1-x)}S_x$	36.06	55.6	0.01	0.07	0.18	0	0	0	2500	2700	0.05	93.12
27 /7	Po	FeS_2	53.37	45.35	0.02	0.01	0	0	0	400	1200	2000	0	99.59
28 /8	Po	FeS_2	52.57	46.66	0.02	0.03	0.01	0.28	0	500	500	800	0	100.45
29 /8	Po	$Fe_{(1-x)}S_x$	38.79	57.91	0	0.03	0.18	0.19	0	300	700	1200	0.03	97.96
30 /9	Py	FeS_2	52.70	46.32	0	0.04	0.04	0.04	0	0	1700	1400	0.05	100.07
31 /9	Po	$Fe_{(1-x)}S_x$	38.27	58.65	0.05	0.05	0.17	0.43	0	1000	100	900	0	98.44
32/10	Po	$Fe_{(1-x)}S_x$	38.87	59.11	0.02	0.06	0.07	0	0	0	1100	2000	0.03	98.83
33/10	Py	FeS_2	52.16	46.41	0.03	0	0.14	0.3	0	0	1500	2800	0	100.08
34/11	Po	$Fe_{(1-x)}S_x$	37.44	58.89	0	0.05	0.17	0.3	100	0	300	1500	0.02	97.69
35/11	Py	FeS_2	53.19	46.78	0.01	0.05	0.02	0.07	0	0	700	3200	0.01	101.22
36/12	Asp	FeAsS	20.37	35.04	0	0.39	0.03	42.88	400	0	1400	600	0.03	99.20
37/12	Asp	FeAsS	20.11	34.7	0	0.15	0	42.39	600	600	0	700	0.02	97.77
38/12	Asp	FeAsS	19.91	35.31	0	0.11	0	42.22	300	0	300	1200	0	97.87
39/13	Po	$Fe_{(1-x)}S_x$	38.56	60.61	0	0.09	0.14	0.09	400	0	800	1800	0.08	100.45
40/13	Po	$Fe_{(1-x)}S_x$	38.01	60.72	0	0.06	0.15	0	0	0	0	300	0	99.50

by Au showing higher values in chalcopyrite, pyrrhotite, and pyrite). Analytical data further show that there is wide variability in invisible gold concentration within sulfides. This might be due to the fluctuating physico-chemical conditions favorable for invisible gold deposition. Other factors such as fugacity of sulfur and redox condition may also have played vital role in invisible gold precipitation (Sahoo 2011).

DISCUSSION AND CONCLUSIONS

Presence of invisible gold within carbonaceous cherty quartzite of the study area has not been reported by previous workers. Gold occurs both in disseminated form and also as invisible gold occurrences or chemically bound gold within sulfides. It may be inferred that during the early stages gold co-precipitated with other sulfides and was

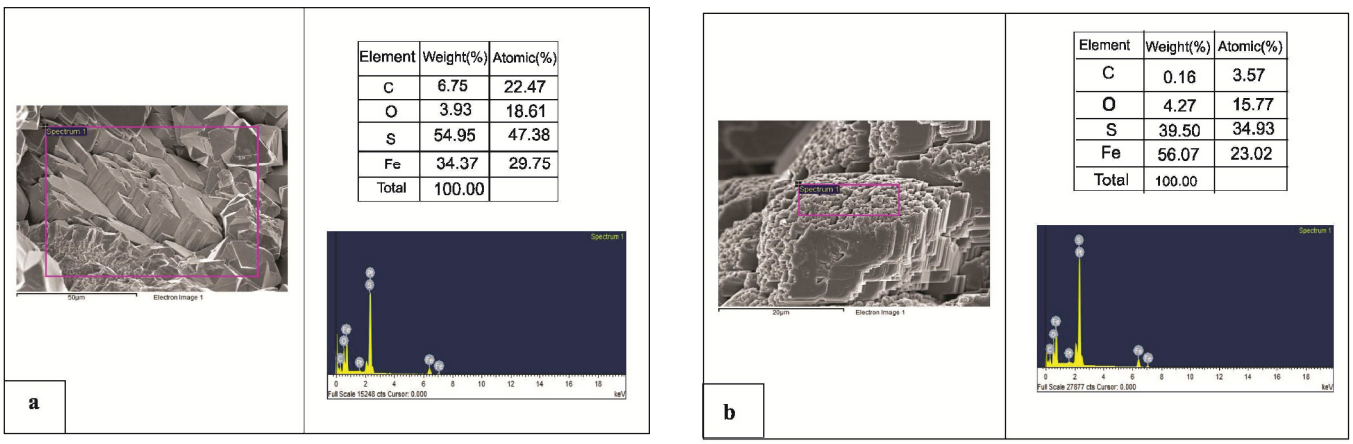

Fig.5. SEM-EDS analysis of ore minerals showing presence of (a) pyrite grains (b) pyrrhotite grains.

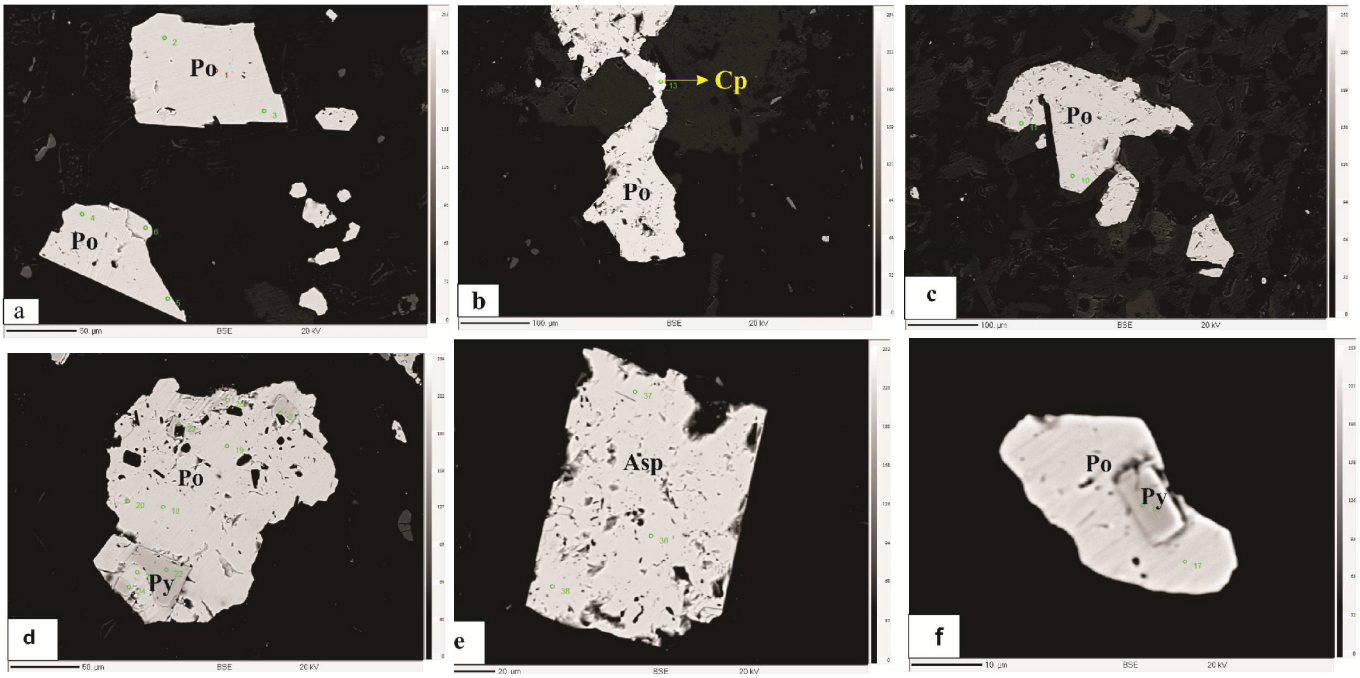

Fig.6. BSE images from EPMA exhibiting various ore minerals which contains invisible gold (a) Pyrrhotite (b) Chalcopyrite replaced pyrrhotite(c) Pyrrhotite (d) Pyrite within pyrrhotite (e) Arsenopyrite (f) cubic pyrite within pyrrhotite.

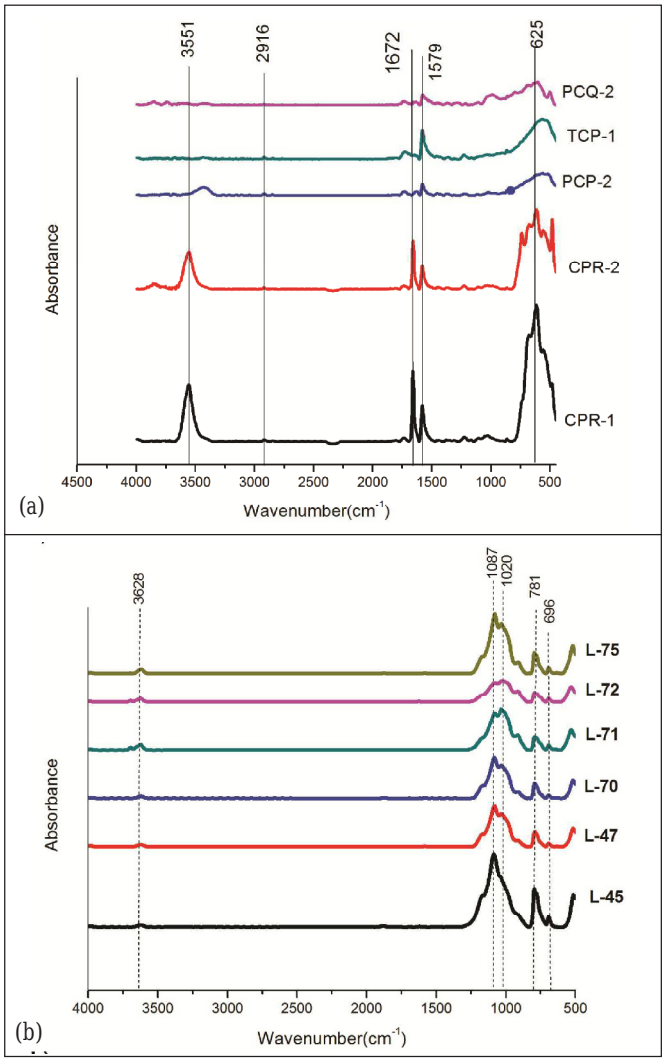

Fig.7. FTIR peaks of carbon bearing rocks showing distinct peaks and functional groups.

locked into crystal lattices of pyrrhotite, pyrite, chalcopyrite and arsenopyrite. Further organic carbon was converted into CO_2 due to the chemical interaction between the water and carbonaceous host rock; effervesced under lower confining pressure in the quartz veins. This may have resulted in the partitioning of H_2S into the vapor phase, which leads to the destabilization of Au bisulfide complex with the aid of shearing and metamorphism affect. The remobilization oflattice bound gold led to the gold occurring as substrate form in second stage. In the final stage, increase in P-T conditions resulted in gold being expelled from sulfides, followed by the precipitation of free gold within the carbonaceous host rocks (Sahoo and Venkatesh 2014; Mukherjee and Venkatesh, 2016). Based on the field relationship and detailed petrographic studies it may be inferred that the gold mineralization within the NSMB is controlled both by structural as well as lithological parameter. Hydrothermal fluid circulation and emplacement through fault may be considered as principal mechanism

Table 2. Total carbon (TC) and total organic carbon (TOC) values of mineralized carbonaceous host rocks from Dalma volcano sedimentary basin.

Sample Number	Total Carbon (wt%)	Total organic carbon (TOC)	Inorganic carbon
CSP-1	5.8136	5.7283	0.0853
RCP-1	3.8029	3.7237	0.0792
CPT-1	4.0245	4.0182	0.0063
L-20	1.1732	1.084	0.0892
L-30	0.739	0.697	0.042
L-31	6.7405	6.5025	0.238
L-33	0.065	0.022	0.043
L-37	0.877	0.616	0.261
L-40	7.3776	6.9875	0.3901
L-41	3.655	3.448	0.207
L-45	3.6161	3.5149	0.1012
L-60	4.3568	1.7308	2.626
L-63	4.3815	1.6229	2.7586
L-69	4.603	4.318	0.285
L-70	4.948	4.537	0.411
L-71	4.244	4.152	0.902

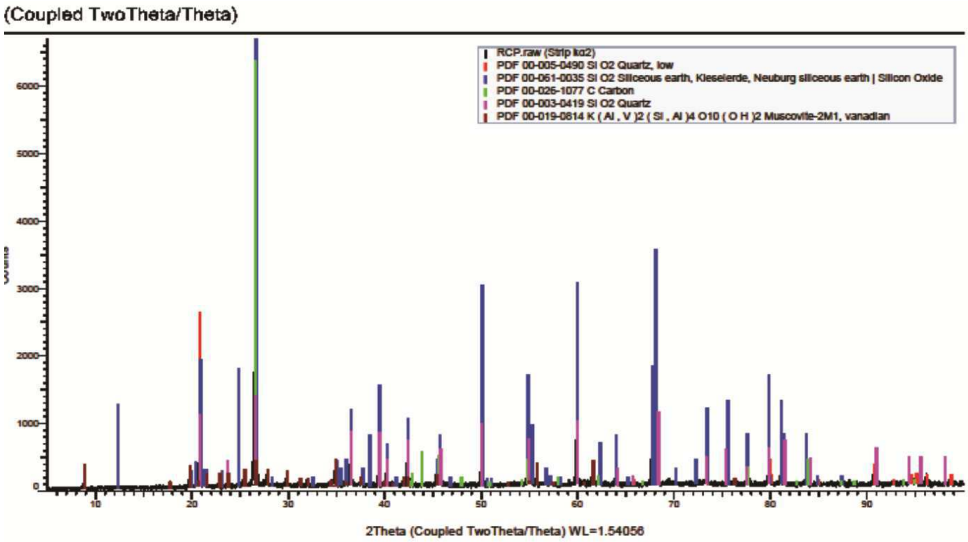

Fig.8. XRD peaks showing carbon, quartz and clay groups of minerals.

for gold transportation and their deposition. The organic carbon may be held responsible to provide the necessary reducing environment during mineralization process. Presence of organic carbon is well evident by the FTIR, HR-XRD and TOC analysis. Further studies related to characterization and understandings of invisible gold occurrences may help in the exploration of gold prospects within the study area.

Acknowledgements: The authors are thankful to IIT (ISM) for providing financial support and also for Central Research Facility (CRF) from where EPMA and SEM analysis were carried out. Authors are acknowledging infrastructural facility provided by Department of Applied Geology, ISM, Dhanbad. Authors are also thankful for SAIF-IITB for carrying out FTIR analysis, Dr. Sanchita Chakravarty, Scientist at CSIR-National Metallurgical Laboratory, Jamshedpur for availing facility of TOC analysis at her laboratory and Indian Association for Cultivation of Science for carrying out HR-XRD analysis.

References

Ashley, P.M., Creagh, C.J., Ryan, C.G. (2000) Invisible Gold in Ore and Mineral Concentrates from the Hillgrove Gold-Antimony Deposits, NSW, and Australia. Mineralium Deposita, v.35, pp.285-301

Bhattacharya, H.N., Mahapatra, S. (2008) Evolution of the Proterozoic Rift Margin Sediments, North Singhbhum Mobile Belt, Jharkhand-Orissa, India. Precambrian Res., v.162, pp.302-316

Bhattacharya, D.S., Dasgupta, D. (1979) Chemical Clues to the Origin of Basic Fragments Embedded in a Basaltic Suite of the Precambrian Metamorphic Terrain of Singhbhum, Eastern India. Contib. Mineral. Petrol., v.71, pp.177-183.

Bose, M.K., Chakraborti, M.K., Saunders, A.D. (1989)Petrochemistry of the Lavas from Proterozoic Dalma Volcanic Belt, Singhbhum, Eastern India. Geologische Rundschau, v.78(2), pp.633-648.

Boyle, R.W. (1980), The Geochemistry of Gold and its Deposits. Geol. Surv. Canada Bull., pp.1-533.

Boyle, R.W. (1987) Gold: History and Genesis Of Deposits: Van Nostrand-Reinhold Company, New York, pp.583-585

Bürg, G.H. (1930) Die Sichtbarmachung Des Feinverteilten Goldes In Goldhaltigen Erzen Und Ihre Wirtschaftliche Bedeutung. Metall und Erz, v.27, pp.333-338.

Cabri, L.J., Chryssoulis, S.L., Devilliers, J.P.R., Laflamme, J.H.G., Buseck, P.R. (1989) The Nature of "Invisible" Gold in Arsenopyrite: Canadian Mineral., v.27, pp.353-362.

Cabri, L.J., Chryssoulis, S.L.,Campbell, J.L., Teesdale, W.J. (1991) Comparison of In-Situ Gold Analyses in Arsenian Pyrite. Appld. Geochem., v.6, pp.225-230.

Cathelineau, M., Boiron, M.C., Holliger, P., Marion, P., Denis, M.(1989) Gold in Arsenopyrites:Crystal Chemistry, Location and State, Physical and Chemical Conditions of Deposition. Econ. Geol., v.6, pp.328-341

Chakraborti, M.K. (1980) On the Pyroclastic Rocks of Dalma Volcanic Sequence, Singhbhum, Bihar. Indian Jour. Earth Sci., v.7, pp.216-222.

Chakraborti, M.K., Bose, M.K. (1985)Evaluation of the Tectonic Setting of Precambrian Dalma Volcanic Belt, Eastern India Using Trace Element Data. Precambrian Res., v.28, pp.253-268.

Chatterjee, P., De.S., Ranaivoson, M., Mazumder, R., Arima, R. (2013) A Review of the ~1600 Ma Sedimentation,Volcanism and Tectono-Thermal Events in The Singhbhum Craton, Eastern Indian Craton. Geoscience Frontiers, v.4, pp.277-287.

Chen, Y., Mastelerz, M., Schimmelmann, A. (2012) Characterization of chemical functional groups in macerals across different coal ranks via Micro-FTIR Spectroscopy. Internat. Jour. Coal Geol., v.104, pp.22-33.

Cook, N.J., Chryssoulis, S.L. (1990) Concentrations of "Invisible" gold in the Common Sulfides. Canadian Mineral., v.28, pp.1-16.

Dunn, J.A. (1929) Geology of North Singhbhum Including Parts of Ranchi and Manbhum Districts. Mem. Geol. Surv. India, v.54, pp.1-166.

Dunn, J.A., Dey, A.K. (1942)The Geology and Petrology of Eastern Singhbhum and Surrounding Areas. Mem. Geol. Surv. India, v.69(2), pp.281- 456.

Errikson, P.G., Mazumder, R., Sarkar, S., Bose, P.K., Altermann, W., Van Der Merwee, R. (1999) The 2.7-2.0 Ga Volcano-Sedimentary Record of Africa, India and Australia: Evidence for Global and Local Changes in Sea Level and Continental Freeboard. Precambrian Res., v.97, pp.269-302.

Friedl, J., Wagner, F.E., Wang, N. (1995) On the Chemical State of Combined Gold in Sulfidic Ores. Conclusions from Mo¨Ssbauer Source Experiments. Neu. Jah. fur Mineralogie, Abhandlungen, v.169, pp.279-290.

Fleet, M.E. and Mumin, A.H. (1997) Gold-Bearing Arsenian Pyrite, Marcasite and Arsenopyrite from Carlin Trend Gold Deposits and Laboratory Synthesis. American Mineral., v.82, pp.182-193

Galley, A.G., Hannigton, M.D., Jonasson, I.R. (2007)Volcanogenic Massive Sulphide Deposits. *In:* Goodfellow, W.D., (Ed.), Mineral Deposits of Canada: A Synthesis of Major Deposits Types, District Metallogeny, The Evolution of Geological Province and Exploration Methods. Geol. Assoc. Canada. Mineral Deposits Division, Spec. Publ., v.5, pp.141-161.

Genkin, A.D., Bortnikov, N.S., Cabri, L.J., Wagner, F.E., Stanley, C.J., Safonov, Y.G., Mcmahon, G., Friedl, J., Kerzin, A.L., Gamyanin, G.N. (1998) A Multidisciplinary Study of Invisible Gold in Arsenopyrite from Mesothermal Gold Deposits in Siberia, Russian Federation. Econ. Geol., v.93, pp.463-487.

Gupta, A. , Basu, A., Ghosh, P.K. (1980) The Proterozoic Ultramafic and Mafic Lavas and Tuffs of the Dalma Greenstone Belt, Singhbhum, Eastern India. Canadian Jour. Earth Sci., v.17, pp.210-231.

Gupta, A., Basu, A., Ghosh, P.K. (1982) Ultramafic Volcaniclastics of the Precambrian Dalma Volcanic Belt, Singhhum, Eastern India. Geol. Magz., v.119, pp.505-510.

Gupta,A., Basu,A. (2000) North Singhbhum Proterozoic Mobile Belt, Eastern India-A review. Geol. Surv. India Spec. Publ., v.55, pp.195-226.

Hough, R.M., Noble, R.R.P., Reich, M. (2011) Natural Gold Nanoparticles. Ore Geol. Rev., v.42, pp.55-61.

Jha, V., Singh, S., Venkatesh, A.S. (2015) Invisible Gold Occurrence within the Quartz Reef Pyrite of Babaikundi Area, North Singhbhum Fold and Thrust Belt, Eastern Indian Shield: Evidences from Petrographic, SEM and EPMA Studies. Ore Geol. Rev., v.65, pp.426-432.

Keith, M., Hackle, F., Haase, K.M., Schampera, U.S., Klemd, R. (2016) Trace Element Systematic of Pyrite from Submarine Hydrothermal Vent. Ore Geol. Rev., v.72, pp.728-745.

Large, R.R., Danyushevsky, L., Hollit, C., Maslennikov, V., Meffre, S., Gilbert, S., Bull, S., Scott, R., Emsbo, P., Thomas, H., Singh, B., Foster, J. (2009) Gold and Trace Element Zonation in Pyrite Using a Laser Imaging Technique: Implications for the Timing of Gold in Orogenic and Carlin-Style Sediment-Hosted Deposits. Econ. Geol., v.104, pp.635-668

Li, J., Daming, F., Jeng, Q., Guilan, Z. (1994) The Existence of Negative Valence State of Gold in Sulfide Minerals and its Formation Mechanism [Abs]. International Mineralogical Association, General Meeting, 16th Pisa Sept 4-9, 1994, Abstracts, pp.219-236

Maddox, M., Bancroft, G.M., Scaini, M..J, Lorimer, J.W. (1998) Invisible Gold: Comparison of Au Deposition on Pyrite and Arsenopyrite. American Mineral., v.83, pp.1240-1245

Mahadevan, T.M. (2002) Geology of Bihar and Jharkhand. Geological Society of India, Bangalore, pp.169-192, 193-230.

Mahato, S., Goon, S., Bhattacharya, A., Mishra, B., Bernhardt, Heinz, J. (2008) Thermotectonic Evolution of the North Singhbhum Mobile Belt (Eastern India): A View from the Western Part of the Belt.Precambrian Res., v.162, pp.102-127.

Maurya, V.P., Shalivahan, Bhattacharya, B.B., Adhikari, P.K., Das, L.K. (2015) Preliminary Magnetotelluric Results across Dalma Volcanic, Eastern India: Inferences on Metallogeny. Jour. Appld. Geophys., v.115, pp.171-182.

Mazumder, R. (2000) Turbulance-Particle Interactions and their Implications for Sediment Transportand Bedform Mechanics under Unidirectional Current; Some Recent Developments. Earth Sci. Rev., v.50, pp.113-124.

Mazumder, R. (2003) Correlations between the Eastern Block of the North China Craton and the South Indian Block of the Indian Shield:An Archaean to Paleoproterozoic Link-Comment. Precam. Res., v.127, pp.379-380.

Mazumder, R. (2005) Proterozoic Sedimentation and Volcanism in the Singhbhum Crustal Province, India and their Implications. Sediment. Geol., v.176, pp.167-193.

Misra, S., Johnson, P.T. (2005) Geochronological Constraints on Evolution of Singhbhum Mobile Belt and Associated Basic Volcanics of Eastern Indian Shield. Gondwana Res., v.8(2), pp.129-142

Mukherjee, R., Venkatesh, A.S. (2016) Albititte hosted gold-sulfide mineralization: An example from the Paleoproterozoic Aravalli supracrustal Sequence, Bhukia Area, Western India. Episodes, v.39(4), pp.590-598.

Mukherjee, A., Basu, S., Manna, P. K., Yusuf, S.M. and Pal, M. (2014) Giant Magnetodielectric and Enhanced Multiferroic Properties of Sm Doped Bismuth Ferrite Nanoparticles. Jour. Materials Chemistry. C, v.2, pp.5885-5891.

Mukhopadhaya, D. (1999) Precambrian Plate Tectonics in the Eastern Indian Shield. *In:* Synchanthavog, S.P.H. (Ed.), Custal Evolution And Orogeny. Oxford IHB Publ. Co., pp.75-100.

Mukhopadhaya, D. (1994) Evolution of the Precambrian Terrane of Singhbhum. Extended Abstract, Symp on Mantle Dynamics and its Relation to Earthquakes and Volcanism, Calcutta, pp.45-48.

Mumin, A.H., Fleet, M.E., Chryssoulis, S.L.(1994) Gold Mineralization in As-Rich Mesothermal Gold Ores of the Bogosu-Prestea Mining District of the Ashanti Gold Belt, Ghana; Remobilization of "Invisible" Gold. Mineralium Deposita, v.29, pp.445-460.

Okolo, G.N., Neomagus, H.W.J.P., Everson, R.C., Roberts, M.J., Bunt, J.R., Sakurorvs, R., Mathews, J.P. (2015) Chemical-Structural Properties of South African Bituminous Coals: Insights from Wide Angle XRD-Carbon Fraction Analysis, ATR-FTIR, Solid State ^{13}C NMR, HRTEM Techniques. Fuel, v.158, pp.779-792.

Pal, D.C., Robert, B., Trumbull, Wiedenbeck, M. (2010) Chemical and Boron Isotope Composition of Tourmaline from the Jaduguda U(-Cu-Fe) Deposit, Singhbhum Shear Zone, India: Implications for the Sources and Evolution of Mineralizing Fluids. Chemical Geol., v.277, pp.245-260

Pal, T., Deb, M. (2013)Chert Associated in the Mineralized Zone of the Paleoproterozic Dariba-Rajpura-Bethumni Belt, Rajasthan: An Oxygen Isotope Study and its Implication. Curr. Sci., v.105(1).

Palenik, C.S., Utsunomiya, S., Reich, M., Kesler, S.E., Wang, L., Ewing, R.C. (2004) "Invisible" Gold Revealed: Direct Imaging of Gold Nanoparticles in a Carlin-Type Deposit. American Mineral., v.89, pp.1359-1366.

Prasad,S.R., Singh, U.P., Sharma, A.K., Das, S.K. (1994) Progress Report on Preliminary Search for Gold Base Metal and Other Noble Metal in Dalma Volcanic and Singhbhum Metasedimentary Rocks around Rudiya-Kantaldih In Parts of Singhbhum Districts, Bihar (73 J/1), Progress Report for the Field Season 1992-1993.

Roy, A., Sarkar, A., Jeyakumar, S., Aggarwal,S.K., Ebihara, M. (2002b) Mid-Proterozoic Plume Related Thermal Event in Eastern Indian Craton: Evidence from Trace Elements, REE Geochemistry and Sr-Nd Isotope Systematic Of Basic-Ultrabasic Intrusive from Dalma Volcanic Belt. Gondwana Res., v.5, pp.133-146.

Russell, J.D. (1987) Infrared Methods, *In:* A Handbook of Determinative Methods in Clay Mineralogy Wilson M.J. (Ed.), London, Blackie, pp. 133-173.

Saha, I., Venkatesh, A.S. (2002) Invisible Gold within Sulfides from Archean Hutti-Maski Schist Belt, Southern India. Jour. Asian Earth Sci., v.20, pp.449-457.

Sahoo, P.R. (2011)Metallogenetic Aspects of Gold Mieralization in and around Kundarkocha Area of the Singhbhum Orogenic Belt, Eastern India, Ph.D thesis (unpublished), ISM, Dhanbad-826004, pp.106-110.

Sahoo, P.R., Venkatesh, A.S. (2014) "Indicator" Carbonaceous Phyllite/ Graphitic Schist in the Archean Kundarkocha Gold Deposit, Singhbhum Orogenic Belt, Eastern India: Implication for Gold Mineralization vis-a-vis Organic Matter. Jour. Earth System Science, v.123(7), pp.1693-1703.

Simon, G., Kesler, S.E., Chryssoulis, S. (1999) Geochemistry and textures of gold-bearing arsenian pyrite, Twin Creeks, Nevada: Implications for deposition of gold in Carlin-type deposits. Econ. Geol., v.94, pp.405-421.

Singh, S.P. (1997) Geochemistry of Acid Volcanics of the Dalma Group, Singhbhum, Eastern India. Jour. Geol. Soc. India, v.49, pp.437-441.

Singh,S.P. (1998) Precambrian Stratigraphy of Bihar. *In:* Paliwal, B.S., (Ed.), The Indian Precambrian. Jodhpur, India: Scientific Publ., pp.376-408.

Tarnocai, C.A., Hattori, K., Cabri, L.J. (1997) "Invisible" Gold in Sulfides from Campbell Mine, Red Lake Greenstone Belt, Ontario: Evidence for Mineralization During Peak Metamorphism. Canadian Mineral., v.35, pp.805-815.

Vandenbroucke, M. (2003) Kerogen: from Types of Models of Chemical Structure. Oil & Gas Science and Technology, v.58(2), pp.243-269.

Walsh, M.M., Lowe,D.R.(1999) Modes of Accumulation of Carbonaceous Matter in Early Archaen: A Petrographic and Geochemical Study of the Carbonaceous Chert of Swaziland Supergroup. Geol. Soc. Amer., Spec. Paper 329.

Wan,B., Zhang, L., Xiao,W. (2010)Geological and Geochemical Characteristics and Ore Genesis of Keketale VMS Pb-Zn Deposits, Southern Altai Metallogenic Belt, NW China. Ore Geology Rev., v.37,pp.114-126.

Yang, S., Blum, N., Rahders, E., Zhang, Z. (1998) The Nature of Invisible Gold in Sulfides from the Xiangxi Au-Sb-W Ore Deposit in Northwestern Hunan, People's Republic of China. Canadian Mineral., v.36, pp.1361-1372.

Yellur, D.D. (1977) Geochemical Clues In The Investigation of the Tectonic Environment of the Dalma Greenstone, Bihar, India. Chemical Geol., v.20, pp.345-363.

Zhang, M., Reilly, S.Y.O., Wang, K.I., Honsky, J., Griffin,W.L. (2008)Flood Basalts and Metallogeny: The Lithospheric Mantle Connection. Earth Sci. Rev., v.86, pp.145-174.

(Received: 31 July 2017; Revised form accepted: 7 November 2017)